Aromatic-Exfoliated Transition Metal Dichalcogenides: Implications for Inherent Electrochemistry and Hydrogen Evolution

Shu Min Tan,[a] *Zdeněk Sofer,*[b] *Jan Luxa,*[b] *Martin Pumera*[a]*

[a] School of Physical and Mathematical Sciences, Division of Chemistry and Biological Chemistry, Nanyang Technological University, 21 Nanyang Link, 637371 Singapore.

[b] Department of Inorganic Chemistry, University of Chemistry and Technology Prague, Technická 5, 166 28 Prague 6, Czech Republic.

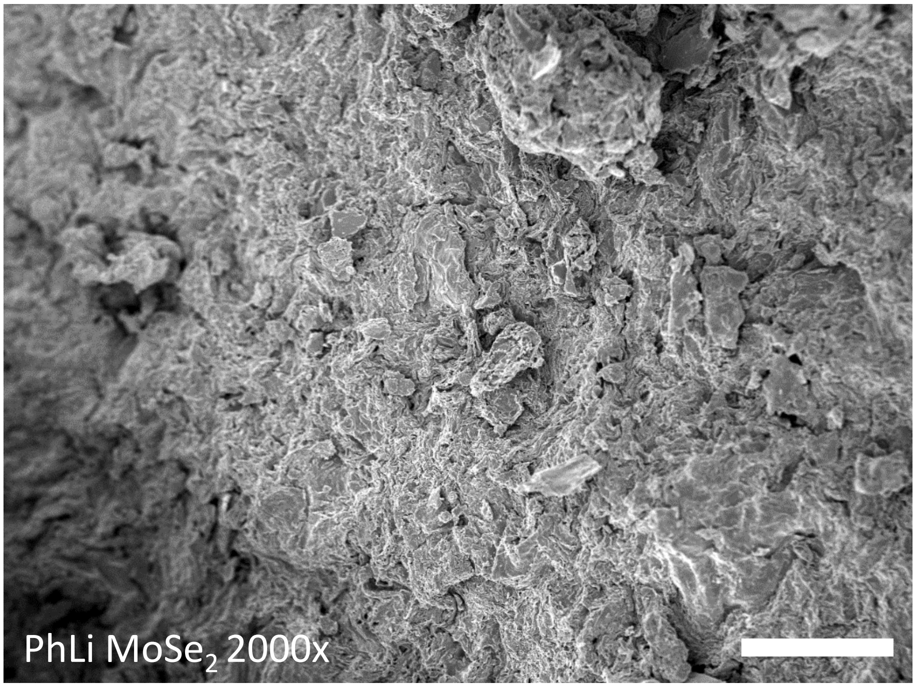

Figure S1 Scanning electron micrograph of $MoSe_2$, after treatment with phenyllithium, followed by exfoliation in water. Scale bar represents 10 μm.

Table S1 Full width at half maximum (fwhm) values of E_{2g} and A_{1g} peaks of MoS_2, $MoSe_2$, WS_2, and WSe_2, together with the corresponding peak separations.

Material	fwhm (cm^{-1}) E_{2g}	A_{1g}	Peak separation between E_{2g} and A_{1g} (cm^{-1})[c]
Bulk MoS_2	6.3	7.0	25.8
PhLi MoS_2	7.7	8.0	25.4
Naph MoS_2	10.2	10.7	25.0
Anth MoS_2	9.5	9.8	24.8
Bulk $MoSe_2$[a]	-	6.5	43.1
PhLi $MoSe_2$[a]	-	8.1	44.2
Naph $MoSe_2$[a]	-	19.4	49.1
Anth $MoSe_2$[a]	-	7.7	45.0
Bulk WS_2	13.2	6.6	70.0
PhLi WS_2	14.2	8.1	68.7
Naph WS_2	7.9	8.5	64.2
Anth WS_2	12.9	10.6	63.9
Bulk WSe_2[b]	11.7		-
PhLi WSe_2[b]	17.9		-
Naph WSe_2[b]	23.8		-
Anth WSe_2[b]	42.3		-

[a] The signal-to-noise ratio of E_{2g} peak of $MoSe_2$ is low for determination of its fwhm.

[b] The E_{2g} and A_{1g} peaks of WSe_2 overlap, rendering the peak separation indeterminate. The fwhm provided are of the overlapped E_{2g}/A_{1g} peaks of WSe_2.

[c] The differing exfoliation efficiencies derived from the Raman spectroscopy (based on E_{2g}–A_{1g} peak separation) and surface area measurements are likely due to the utilization of different solvents for sample preparation (DMF for Raman spectroscopy and deionized water for methylene blue adsorption), which is limited by the suitability of their properties for the technique used. However, since TMD dispersions in DMF were used for all measurements except for methylene blue adsorption, the Raman spectroscopy data is expected to be more illustrative of the relationship between the extent of exfoliation and the intercalant used, compared to the surface area measurements.

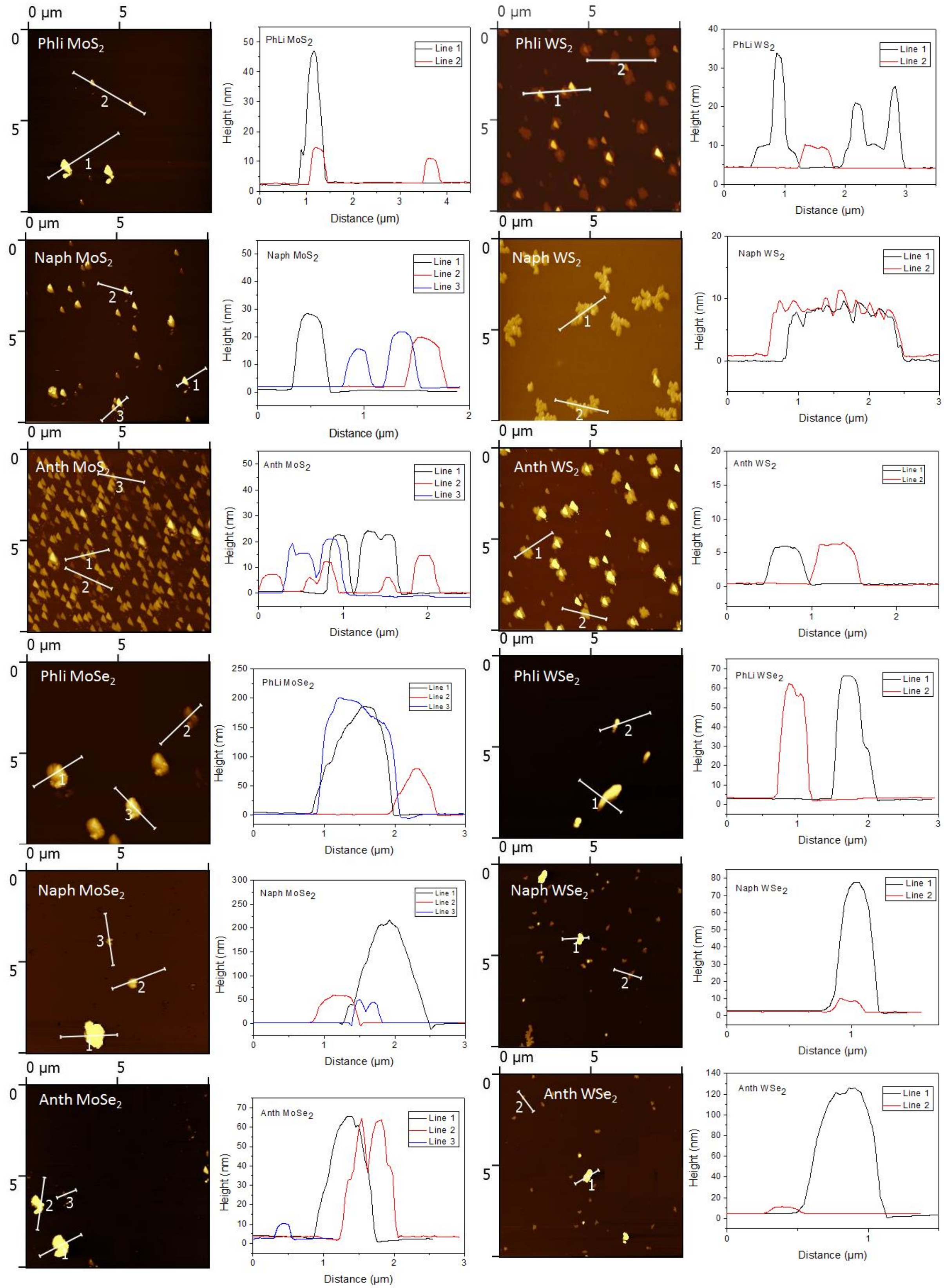

Figure S2 AFM measurements and corresponding height profiles of exfoliated MoS_2, $MoSe_2$, WS_2, and WSe_2.

Table S2 1T/2H ratios of MoS_2, $MoSe_2$, WS_2 and WSe_2 in the bulk state and after treatment with phenyllithium, sodium naphthalenide or sodium anthracenide, followed by exfoliation in water, obtained from XPS data.

1T/2H ratio	Materials			
	MoS_2	$MoSe_2$	WS_2	WSe_2
Bulk	0	0.205	0.108	0
PhLi	0.367	1.002	4.369	0.921
Naph	0.406	0.709	3.485	0.987
Anth	0.156	0.258	0.678	0

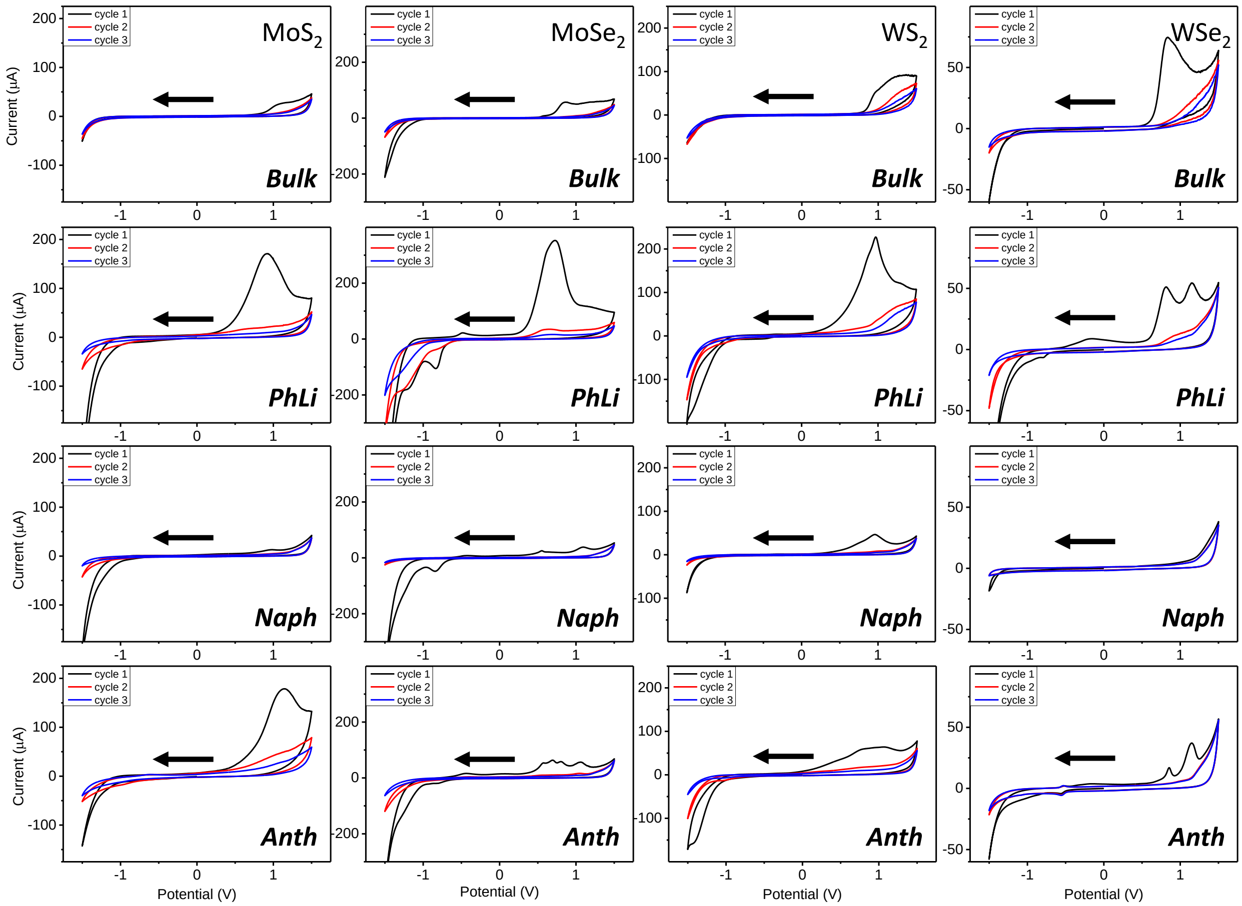

Figure S3 Inherent electrochemistry of (left to right) MoS_2, $MoSe_2$, WS_2, and WSe_2, (top to bottom) untreated and after treatment with phenyllithium, sodium naphthalenide or sodium anthracenide, followed by exfoliation in water. Each measurement was run for three cycles (as indicated), with the starting potential at 0 V. The arrows denote the initial scan direction and the y-axes were scaled to a uniform range for each TMD. Conditions: scan rate of 100 mV s^{-1}, phosphate buffer solution (50 mM, pH 7.2) as electrolyte, purged with N_2.

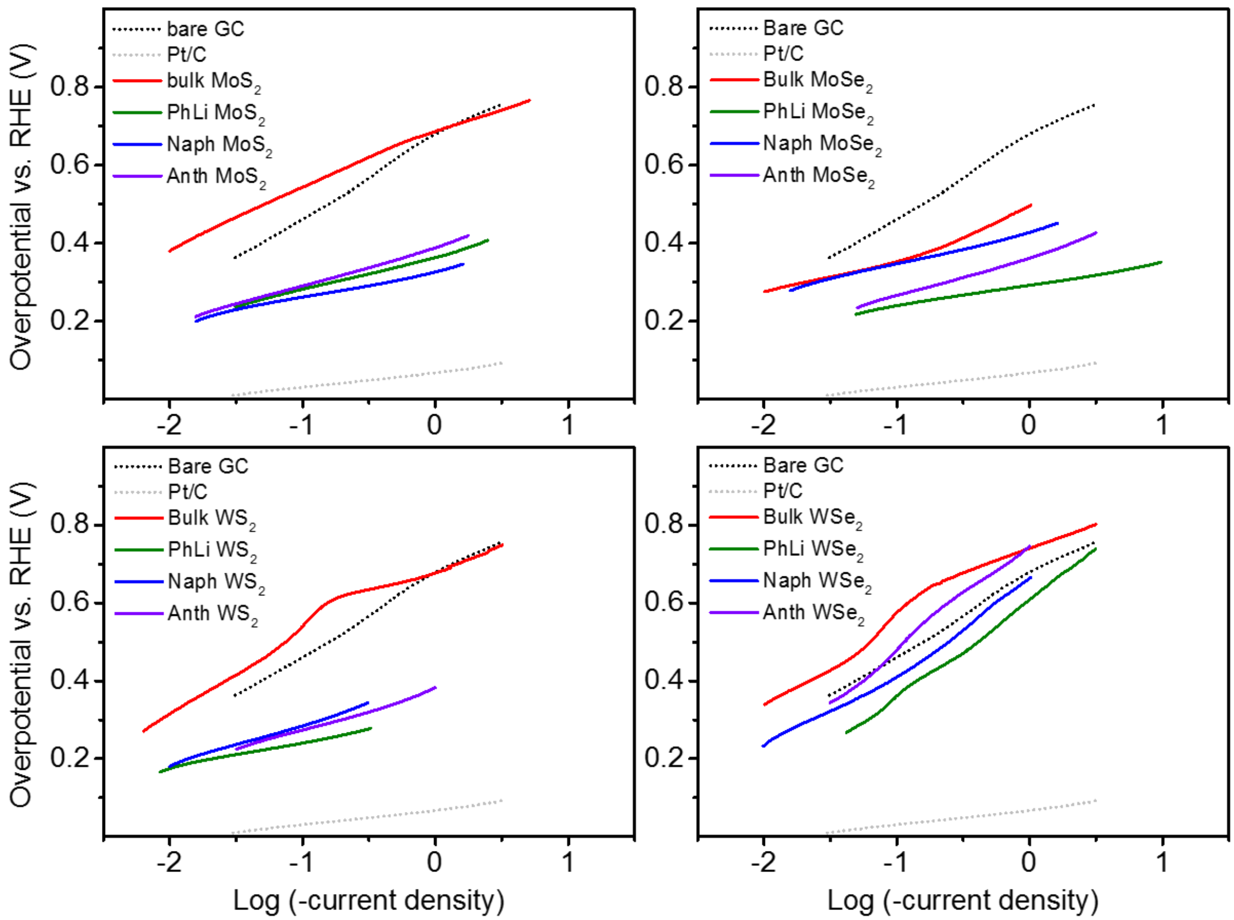

Figure S4 Plots of Tafel slopes of MoS_2, $MoSe_2$, WS_2, and WSe_2, untreated and after treatment with phenyllithium, sodium naphthalenide or sodium anthracenide, followed by exfoliation in water, together with those of Pt/C (grey, dotted) and bare GC electrode (black, dotted).

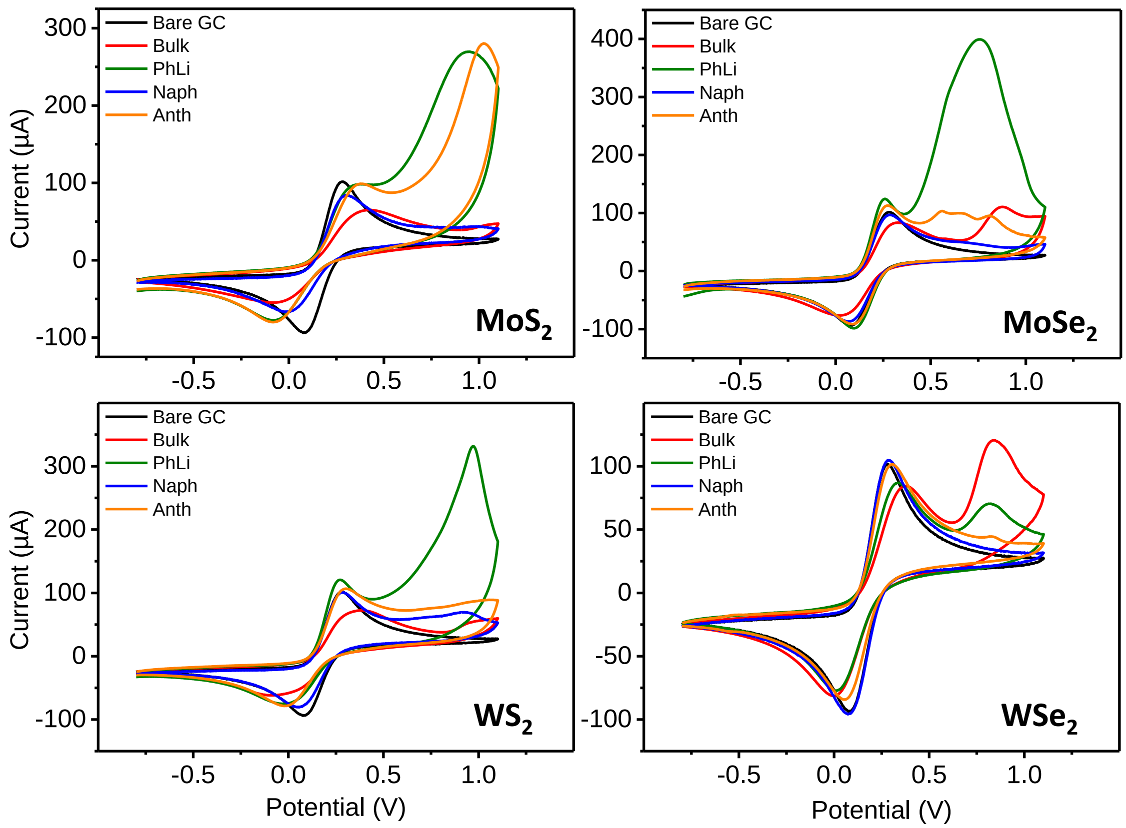

Figure S5 Cyclic voltammograms of $Fe(CN)_6^{4-/3-}$ on MoS_2, $MoSe_2$, WS_2, and WSe_2, as indicated, untreated and after treatment with phenyllithium, sodium naphthalenide or sodium anthracenide, followed by exfoliation in water, as well as that of bare GC. Conditions: 10 mM $Fe(CN)_6^{4-/3-}$, scan rate of 100 mV s^{-1}, 50 mM phosphate buffer solution (pH 7.2) as supporting electrolyte, purged with N_2.

Table S3 Calculated heterogeneous electron transfer rate constant (k^0_{obs}) for $Fe(CN)_6^{4-/3-}$ on MoS_2, $MoSe_2$, WS_2 and WSe_2 in the bulk state and after treatment with phenyllithium, sodium naphthalenide or sodium anthracenide, followed by exfoliation in water. The k^0_{obs} value of bare glassy carbon (GC) is also shown for reference.

k^0_{obs} (cm s^{-1})	Materials				
	MoS_2	$MoSe_2$	WS_2	WSe_2	Bare GC
Bulk	2.94×10^{-5}	2.96×10^{-4}	4.37×10^{-5}	1.10×10^{-4}	1.24×10^{-3}
PhLi	2.84×10^{-5}	1.21×10^{-3}	1.12×10^{-4}	1.06×10^{-4}	-
Naph	2.18×10^{-4}	7.01×10^{-4}	6.25×10^{-4}	1.14×10^{-3}	-
Anth	2.71×10^{-5}	1.23×10^{-3}	1.03×10^{-4}	6.15×10^{-4}	-

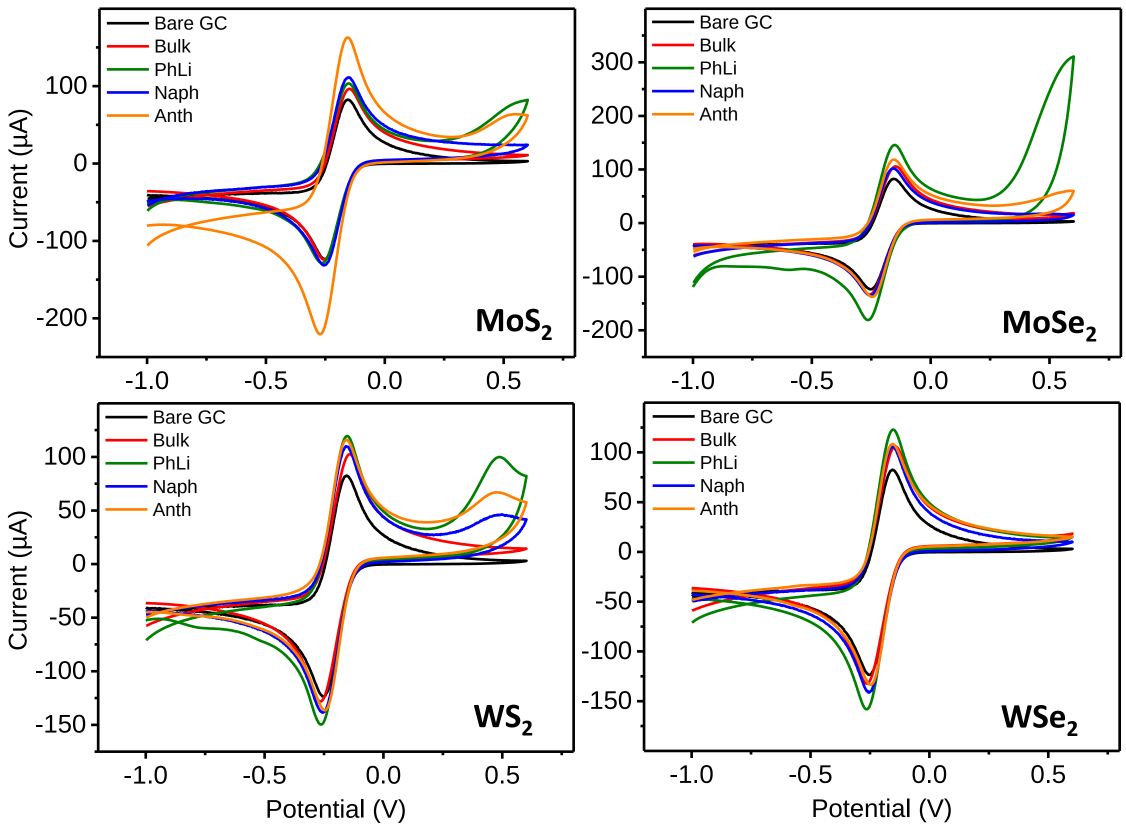

Figure S6 Cyclic voltammograms of $Ru(NH_3)_6^{2+/3+}$ on MoS_2, $MoSe_2$, WS_2 and WSe_2, as indicated, untreated and after treatment with phenyllithium, sodium naphthalenide or sodium anthracenide, followed by exfoliation in water, as well as that of bare GC. Conditions: 10 mM $Ru(NH_3)_6^{2+/3+}$, scan rate of 100 mV s^{-1}, 50 mM phosphate buffer solution (pH 7.2) as supporting electrolyte, purged with N_2.

Table S4 Calculated heterogeneous electron transfer rate constant (k^0_{obs}) for $Ru(NH_3)_6^{2+/3+}$ on MoS_2, $MoSe_2$, WS_2 and WSe_2 in the bulk state and after treatment with phenyllithium, sodium naphthalenide or sodium anthracenide, followed by exfoliation in water. The k^0_{obs} value of bare glassy carbon (GC) is also shown for reference.

k^0_{obs} (cm s^{-1})	Materials				
	MoS_2	$MoSe_2$	WS_2	WSe_2	Bare GC
Bulk	4.38×10^{-3}	4.28×10^{-3}	3.90×10^{-3}	3.97×10^{-3}	5.16×10^{-3}
PhLi	4.18×10^{-3}	4.05×10^{-3}	4.19×10^{-3}	4.12×10^{-3}	-
Naph	4.82×10^{-3}	5.10×10^{-3}	4.99×10^{-3}	4.83×10^{-3}	-
Anth	3.91×10^{-3}	5.76×10^{-3}	5.69×10^{-3}	5.45×10^{-3}	-